JOURNAL OF GEOPHYSICAL RESEARCH, VOL. 102, NO. A8, PAGES 17,649-17,657, AUGUST 1, 1997

An analytic approach to toroidal eigen mode

A. K. Sinha and R. Rajaram

Indian Institute of Geomagnetism, Mumbai

Abstract. It has been shown that the failure of the classical WKB approach in reproducing the correct frequency spectrum and spatial structures of field line resonances should be attributed to the inability of the method to provide a natural solution close to the turning points. A direct analytic solution has been formulated to derive the toroidal field line resonance structure. Finally, the solutions thus obtained have been compared with the numerically found exact solutions in order to test the authenticity of the formalism.

1. Introduction

Long-period geomagnetic pulsations are well-observed phenomena in the Earth's magnetosphere. Their existence in the Earth's magnetosphere has been clearly demonstrated by conjugate point and spacecraft observations. It was *Dungey* [1954] who first proposed that these pulsations might be the result of standing Alfven waves being excited on geomagnetic field lines. Later, *Sugiura* [1961] verified that these waves are observed simultaneously at both ends of the same field line showing that these waves were guided along field lines. Finally, with the advent of rapid-run magnetograms, *Nagata et al.* [1963] confirmed the standing nature of these waves by matching them cycle for cycle at the conjugate points. *Cummings et al.* [1969] made extensive observations of long-period waves with the magnetometer on board the geosynchronous satellite ATS 1. They showed that the waves were long-lived and occurred frequently. They also for the first time gave a quantitative estimate of the field line eigen periods by integrating the second-order wave equation numerically. Thus, by the end of 1960 the standing waves on geomagnetic field lines were established observationally, confirming Dungey's idea.

However, no convincing analytic picture of the phenomena of long-period geomagnetic pulsations has been developed so far. It is important to obtain the correct analytic picture of field line resonance for the simple reason that it will provide a better insight into the phenomena, which should prove to be important in more thoroughly understanding the generation mechanism of these pulsations. It would also help to study the coupling of these hydromagnetic waves with the plasma and all those physical phenomena where the field line structures play an important role in a much simplified way. Though *Warner and Orr* [1979] made an attempt in this direction by using the *Mead and Fairfield* [1975] magnetic field model and solved for wave periods by using the WKB approximation to the toroidal wave equation, the result was very poor, particularly for the fundamental mode of oscillation as regards the time period of the wave. *Singer et al.* [1981] attributed the large discrepancy to the breaking down of WKB method since the wavelength of the oscillation is comparable to the scale size of the system. If this arguement were valid, the actual error (not the percentage of error) in the computed spectrum of WKB frequency should improve with increasing harmonic number where the wavelengths are progressively smaller. In section 2.2 we shall note that this does not happen. The problem with the classical WKB method probably lies in the fact that the solution breaks down as we approach the singularities at the turning points where the solution is not finite. Thus the classical WKB method does not provide a natural solution of the problem. We must look for such a solution which is finite and continuous at the turning points.

In this paper an analytic method based on *Langer*'s [1949] approach has been developed which gives an estimate of the eigen period as well as the spatial structures of the toroidal field line oscillations with remarkable improvement over the estimates provided by the WKB method. Like the WKB approximation, this method also provides the solutions in the variational form whose first-order consideration itself gives a fairly good estimate of frequency as well as the spatial structures of electric and magnetic field fluctuations along a field line. Analytically, the present formalism is an improvement over the formal WKB formalism and ensures that the solutions are well behaved near the turning points. The solutions thus obtained are more natural and physical. Henceforth, throughout the paper we call the WKB method as the formal WKB method, and the present method we direct analytical method (DAM).

2. Theory and Analysis

Low-frequency transverse waves in an infinitely conducting, stationary, magnetized plasma with zero pressure are described by the second-order wave equation [*Singer et al.*, 1981] as

Paper number 97JA01039.
0148-0227/97/97JA-01039$09.00

$$\mu_o \rho \frac{\partial^2}{\partial t^2}(\xi_\alpha / h_\alpha) = \frac{1}{h_\alpha^2} \vec{B_o} \cdot \vec{\nabla} \left[h_\alpha^2 \vec{B_o} \cdot \vec{\nabla}(\xi_\alpha / h_\alpha) \right] \quad (1)$$

where μ_o is the magnetic permeability in the vacuum, ρ is the plasma mass density, ξ_α is the plasma displacement perpendicular to the field line, $\vec{B_o}$ is the ambient magnetic field, the parameter α signifies the mode of oscillation and determines the direction $\vec{\alpha}$ of the field line displacement, and h_α is the scale factor for the normal separation between the field lines in the direction $\vec{\alpha}$ and is determined by the ambient magnetic field structure.

We solve (1) under the following assumptions: (1) The ambient magnetic field is dipolar in nature. (2) The time dependence of all the perturbed quantities is of the form exp $[\iota\omega t]$. (3)The field lines are rigidly fixed at their ends in the ionosphere. (4) The density distribution is given by the power law $\rho = \rho_o (r_o/r)^m$, where m is the density index and ρ_o is the proton mass density at r_o, the geocentric distance to the equatorial crossing point of the field line considered, and r is the geocentric distance to the position of interest on the field line.

If s is the distance measured along the field line, then according to the above assumptions (1) takes the following dimensionless form where the variables have been normalized with respect to the equator.

$$-\frac{\Omega^2}{\sin^{2m}\theta} X = \frac{B}{h_\alpha^2} \frac{d}{dS} \left[h_\alpha^2 B \frac{dX}{dS} \right] \quad (2)$$

with

$$S = \frac{s}{R_E}, \ \Omega = \frac{\omega R_E}{V_{Aeq}}, \ X = \frac{\xi_\alpha}{R_E h_\alpha}, \ B = \frac{B_o}{B_{eq}} \quad (3)$$

where R_E is the Earth's radius, V_{Aeq} is the Alfven velocity at the equator, B_eq is the ambient field at the equator, and θ is the colatitude. Once ξ_α is determined, we can obtain the electric and magnetic field perturbations as

$$b_\alpha = h_\alpha B_o \frac{d}{ds} \left(\frac{\xi_\alpha}{h_\alpha} \right) \quad (4)$$

$$E_\beta = \omega \xi_a B_o \quad (5)$$

where $(\vec{B_o}/B_o, \vec{\alpha}, \vec{\beta})$ form a right-handed orthogonal system.

It should be noted that under the dipole approximation h_α, B and B_eq are given as $h_\alpha = L \sin^3\theta$ for the toroidal mode, $h_\alpha = (\sin^3\theta\sqrt{1+3\cos^2\theta_c})/(\sin^3\theta_c\sqrt{1+3\cos^2\theta})$ for the poloidal mode, $B = \sqrt{1+3\cos^2\theta}/\sin^6\theta$, and $B_eq = 0.311/L^3$ Gauss, where the suffix c indicates the value at the conjugate point and $L = 1/\sin^2\theta_c$ is the geocentric distance in Earth radii of the point where the field line crosses the equator.

2.1. Numerical Exact Solution

Equation (2) can be decoupled into two first-order equations

$$\frac{dX}{dS} = \frac{1}{h_\alpha^2 B} Y \quad (6)$$

$$\frac{dY}{dS} = -\frac{\Omega^2 h_\alpha^2}{B \sin^{2m}\theta} X \quad (7)$$

Equations (6) and (7) could be solved numerically by using the second-order Runge-Kutta method, and the frequency ω was obtained by shooting method using the boundary condition that the eigen function X should vanish at the conjugate points. The spatial structures of electric and magnetic field fluctuations obtained by this method were in perfect agreement with that of *Cummings et al.* [1969]. These fluctuations have been plotted along with those obtained by the WKB method and direct analytic method and will be discussed in due course.

2.2. Formal WKB Solution

Equation (2) can be written in standard WKB form [*Wasow*, 1985] by choosing

$$\frac{dv}{dS} = \frac{1}{h_\alpha^2 B} \quad (8)$$

and noting that $h_\alpha = L\sin^3\theta$, L being the geocentric distance in Earth radii of the point where the field line crosses the equator.
Thus (2) can be written as

$$\epsilon^2 \frac{d^2 X}{dv^2} + \Phi(v) X = 0 \quad (9)$$

where $\epsilon = 1/L^2$ and $\Phi(v) = \Omega^2 \sin^{12-2m}\theta$
The solution of (9) in the formal WKB form (which is applicable for $\Phi(v) \neq 0$) up to the first-order correction is given as

$$X = \exp\left[\frac{S_0}{\epsilon} + S_1\right] \quad (10)$$

where $S_0 = \int \sqrt{-\Phi(v)}\, dv$ and $S_1 = -ln[-\Phi(v)]/4$
It turns out that

$$\exp\left[\frac{S_0}{\epsilon}\right] = \exp\left[\pm \iota\omega\tau\right]$$

$$\exp\left[S_1\right] = \exp\left[-\iota\frac{\pi}{4}\right] \sqrt{\frac{V_{Aeq}}{\omega R_E} \frac{1}{\sin^{3-m/2}\theta}}$$

where

$$\tau = \int \frac{ds}{V_A} = \frac{L R_E}{V_{Aeq}} \int_*^\theta \sin^{7-m}\theta\, d\theta$$

The lower limit asterisk denotes any arbitrary point of reference from where the integration has to be carried out.

In order that the displacements simultaneously vanish at the two conjugate points (as required by the boundary conditions adopted in section 2.1), it is necessary that

$$2\omega \int_{-s_c}^{s_c} \frac{ds}{V_A} = 2n\pi$$

where n is a natural number describing the harmonics, and the limits of integration indicate that it is being carried out between the two conjugate points along a field line. The corresponding time period T_A is then

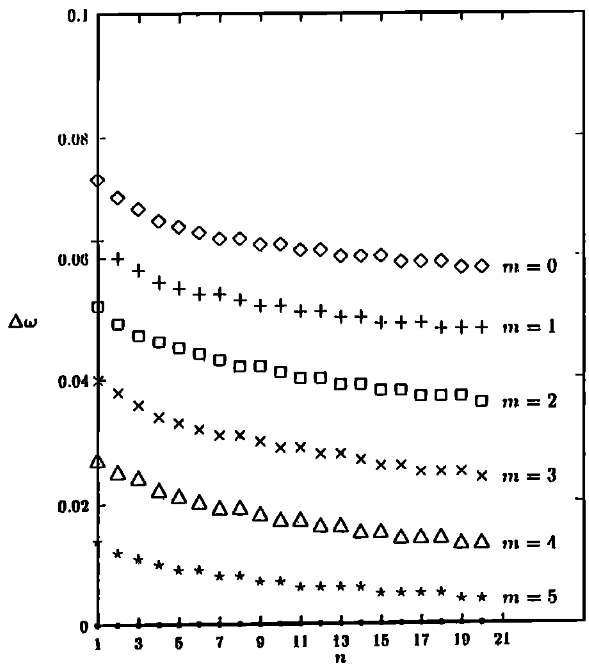

Figure 1. Vriable n is the harmonic number; $\Delta\omega = \omega_{WKB} - \omega_{exact}$ is the difference between the frequencies obtained by formal WKB method and numerical method. The circles on the X axis represent the values for $m = 6$.

given by $T_A = 2\pi/\omega$. Physically, this condition simply means that the resonance will occur only when the time taken by the wave to move from one conjugate point to another and back matches exactly with that required to complete one oscillation for the fundamental and n oscillations for the nth harmonics. The difference between the numerically calculated exact frequency and the WKB frequency of a field line (i.e., for given L) for different values of m has been plotted as a function of harmonic number in Figure 1. It is seen that though the difference is large for lower harmonics, it does not improve appreciably as we progressively go to the higher harmonics. This implies that apart from the wavelength phenomena applicable to lower harmonics as argued by *Singer et al.* [1981] there is something else which is contributing to the discrepancies, otherwise the differences would have considerably decreased in higher harmonics where the wavelength is small compared to the size of the system. Thus the methodology needs to be reexamined thoroughly.

The formal WKB solution up to the first order can be written as

$$X = \frac{1}{\sin^{3-m/2}\theta}\left[A\cos(\omega\tau) + B\sin(\omega\tau)\right] \qquad (11)$$

where the arbitrary constants A and B are to be determined by imposing the condition that the solution is vanishing at the conjugate points.

After the evaluation of the arbitrary constants the solution and its derivative can be written as

$$X = \frac{1}{\sin^{3-m/2}\theta}\left[\cos(\omega\tau) + C\sin(\omega\tau)\right] \qquad (12)$$

$$\frac{dX}{dS} = -\left[\frac{(3-m/2)\cos\theta}{L\sqrt{1+3\cos^2\theta}\sin^2\theta}X + \frac{\omega}{\sin^{3-m/2}\theta}\frac{d\tau}{dS}\left[\sin(\omega\tau) - C\cos(\omega\tau)\right]\right] \qquad (13)$$

where $C = B/A = -\cos(\omega\tau)_{\theta=\theta_c}/\sin(\omega\tau)_{\theta=\theta_c}$

One should note the singularities in the solution at the turning points ($\theta \sim 0, \theta \sim \pi$) where the solution is not finite and the derivative changes sign. These singularities at the turning points have not been accounted for at all in the formal WKB method. As we move away from the equator toward the pole along a field line, it is seen that the solution becomes progressively worse, showing that the solution obtained is not a natural one.

The major problem with the formal WKB method is its inability to handle the singularities at the turning points, that is, ($\theta \sim 0, \theta \sim \pi$). The methodology should be such that we should be able to solve the equation in the complete domain of the independent variable ensuring that the solution is finite and well behaved at the turning points prior to the imposition of the boundary condition. This will provide a more natural solution of the problem. It is this point which has been emphasized in the present work. Using the treatment attributed to *Langer* [1949], the singularities have been taken care of on a purely mathematical basis as described in section 2.3.

2.3. Direct Analytic Method

This method is based on *Langer*'s [1949] approach of tackling the singularity at the turning point. The method ensures that the solution is continuous and well behaved at the points of singularity. The philosophy of the methodology is as follows:

$\Phi(v)$ in (9) is expressed near the turning point in the form $v^r\psi(v)$ as adopted by *Langer* [1949], where r is any real number and the singularity is attributed to v^r, whereas $\psi(v)$ is a well-behaved function. Thus (9) can be written in the *Langer*'s [1949] formalism as

$$\epsilon^2\frac{d^2X}{dv^2} + v^r\psi(v)X = 0 \qquad (14)$$

where $\psi(v)$ is obtained by expanding $\Phi(v)$ around the turning point.

If we integrate (8) by using the condition that $v = 0$ for $\theta = 0$ or π, we get

$$L\,v = 1 \pm \cos\theta \qquad (15)$$

where the plus sign is for the southern hemisphere and the minus sign is for the northern hemisphere.

Equation (15) leads to

$$\sin^{12-2m}\theta = (2L)^r v^r\left[1 - \frac{Lv}{2}\right]^r$$

where $r = 6 - m$

Thus asymptotically, $\psi(v)$ can be written as $\psi(v) = \Phi(v)/v^r$. We therefore see that $\Phi(v)$ in general can be written as $v^r[\Phi(v)/v^r]$, where all the singularities are imparted to v^r and $\psi(v) = \Phi(v)/v^r$ is continuous and well behaved throughout and also at the turning points.

Equation (14) can be written as

$$\left[\frac{d^2}{d\zeta^2} + \frac{\zeta^r}{\epsilon^2} + a^3\frac{d^2a(v)}{dv^2}\right] Z = 0 \qquad (16)$$

by using transformations $X = a(v)Z$, $a(v) \neq 0$, $\zeta = \zeta(v)$, $a(v) = (d\zeta/dv)^{-1/2}$, and $\zeta^r(d\zeta/dv)^2 = v^r\psi(v)$.

In (16) the last term on the left-hand side could be neglected (justification of this has been given in section 2.4) to get the familiar Bessel equation

$$\frac{d^2u}{d\eta^2} + \frac{1}{\eta}\frac{du}{d\eta} + (1 - \frac{\nu^2}{\eta^2})u = 0 \qquad (17)$$

where, $\eta = (2/\epsilon)\zeta^{(r+2)/2}/(r+2)$, $Z = \sqrt{\zeta}u$, and and $\nu = 1/(r+2)$.

Equation (17) is solved separately in the two hemispheres for a typical value of $L = 6.6$ noting that $\eta = (\omega LR_E/V_{Aeq})\int_0^\theta \sin^{7-m}\theta\, d\theta$ for the northern hemisphere, and $\eta = (\omega LR_E/V_{Aeq})\int_\theta^\pi \sin^{7-m}\theta\, d\theta$ for the southern hemisphere. It should be borne in mind that η is symmetric about the equator.

The solution of (17) is a linear combination of Bessel functions of the order of ν and $-\nu$, and hence the solution of (14) could be written as

$$X = \sqrt{\frac{1}{2L\nu}}\sqrt{\frac{V_{Aeq}}{\omega LR_E}}\frac{\eta^{1/2}}{\sin^{3-m/2}\theta}\left[J_\nu(\eta) + K\, J_{-\nu}(\eta)\right] \qquad (18)$$

where $J_\nu(\eta)$ and $J_{-\nu}(\eta)$ are the Bessel functions in the variable η of orders ν and $-\nu$ respectively; and K is an arbitrary constant to be determined from the boundary condition at the conjugate point where the eigen function has to vanish. The symmetry of the solution ensures that K is the same for both the solutions, that is, northern and southern hemispheres. The term containing $J_{-\nu}$ will not appear if we take the boundaries at $\theta = 0$ and $\theta = \pi$. The arbitrary constant K is given as $K = -J_\nu(\eta_{\theta=\theta_c})/J_{-\nu}(\eta_{\theta=\theta_c})$. It can be easily seen that in the vicinity of turning points ($\theta \sim 0, \theta \sim \pi$) the solutions are finite and continuous.

The derivative of X with respect to θ can be written as

$$\frac{dX}{d\theta} = \left[\frac{d\eta}{d\theta}\left[\frac{1}{2\eta} + \frac{d}{d\eta}\log_e\left[J_\nu(\eta) + K\, J_{-\nu}(\eta)\right]\right] - \frac{(3-m/2)}{\tan\theta}\right] X \qquad (19)$$

The continuity of the solution and its derivative at the equator demands that

$$\left[\frac{d}{d\eta}\log_e\left[J_\nu(\eta) + K\, J_{-\nu}(\eta)\right]\right]_{\theta=\frac{\pi}{2}} = -\left[\frac{1}{2\eta}\right]_{\theta=\frac{\pi}{2}} \qquad (20)$$

which is obtained by matching the logarithmic derivative of the solutions in both the hemispheres at the equator.

Plugging the above condition back in (19) shows that the derivative at the equator must be vanishing if the solution does not do so. This is the natural condition for odd harmonics. The condition for even harmonics is that the solution itself is vanishing at the equator. Thus the frequency is determined in a natural and self-consistent way by using the above conditions on the solution and its derivative.

The methodology discussed in this section provides a kind of solution which is continuous and finite at the turning points and on physical ground is a natural solution of the problem of field line resonance. One of the principal aims of the present methodology was to get the correct analytic description for the wave field as one moves along the field line from the equatorial plane to the foot of the field line in the ionosphere. The model can be used to study the effect of density variation of various species on the wave by just making the requisite change in the model. The model can also be used to study the wave structures for different field geometry. The correct analytic structure is also necessary to interpret the pitch angle dependence of the particle fluxes associated with field line resonances in the magnetosphere. This is very important from the physics point of view as particle fluxes are a directly observable physical quantity [*McEntire et al.*, 1985].

2.4. Validity for Neglecting the Last Term in (16)

It was seen that neglecting the term $a^3[d^2a(v)/dv^2]Z$ in (16) is tantamount to adding a term $-(\epsilon^2/a)(d^2a/dv^2)X$ in (14). Thus, solving (16) neglect-

Table 1. Percent Departure of WKB and DAM Frequency From Exact Numerical Frequency

m	HN	WKB, %	DAM, %
5	1	14	3
5	2	6	0.5
4	1	26	6
4	2	11	1
3	1	36	9
3	2	14	1.5
2	1	46	12
2	2	17	2
1	1	54	14
1	2	20	2.5
0	1	61	17
0	2	22	3

The value of m is the density index; HN is the harmonic number.

ing the last term is same as solving the equation

$$\epsilon^2 \frac{d^2X}{dv^2} + \Phi(v)X - \frac{\epsilon^2}{a}\frac{d^2a}{dv^2}X = 0 \qquad (21)$$

This equation was exactly solved by using second-order Runge-Kutta method, and the result was compared with the exact solution of (14). It was seen that even for the worst case, solutions differ by a maximum of 3%. The plot of comparison has been shown in Figure 5.

3. Results and Discussions

A comparison between the numerical exact solution, formal WKB solution, and the direct analytic solution shows that while the formal WKB solution gives a very poor estimate of frequency ω for the fundamental mode, the estimate given by direct analytic method is in fairly good agreement with the numerically found exact frequency. For $m = 6$ the frequency calculated by all three methods and hence the solutions coincide exactly. This is understandable in the sense that for this value of m the singularity disappears and the turning point effect becomes unimportant. This result for $m = 6$ is not at all surprising; because for this value of m the problem reduces to that of a wave on a uniform string. However, it was needed to verify the authenticity of the model. As we take lower values of m, the formal WKB estimate of frequency becomes worse and worse compared to the exact numerical estimate of frequency as shown in Table 1.

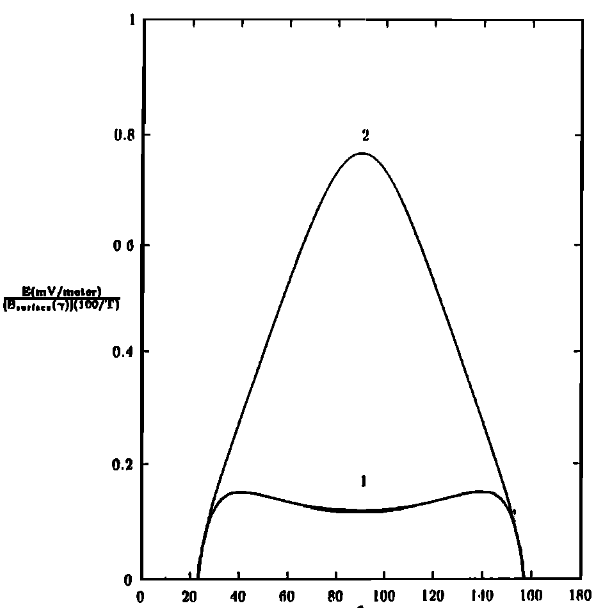

Figure 2a. The fundamental toroidal electric field at any point along the field line for $m = 0$. The value can be obtained from the ordinate by multiplying the indicated factor in which T is the time period of the wave and $B_{surface}$ is the surface magnetic field fluctuation. Solutions obtained by direct analytic method coincide exactly with the numerical exact solution which is indicated by index 1, whereas index 2 describes the solution obtained by formal WKB method.

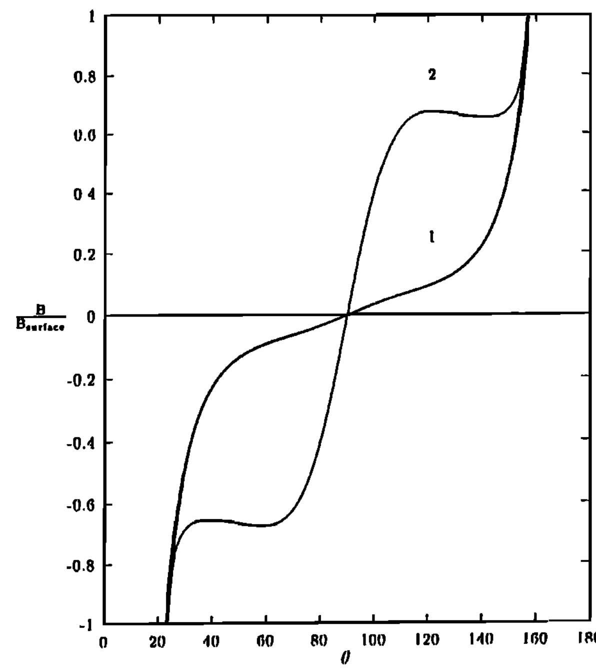

Figure 2b. The fundamental toroidal magnetic field at any point along the field line for $m = 0$. The value can be obtained from the ordinate by multiplying with the factor $B_{surface}$. Solutions obtained by direct analytic method coincide exactly with the numerical exact solution which is indicated by index 1, whereas index 2 describes the solution obtained by formal WKB method.

A singularity at $\theta = 0$ or $\theta = \pi$ results in unrealistically large values of the solutions at the conjugate points which is usually the foot of the field line in the ionosphere (if it is assumed to be perfectly conducting).

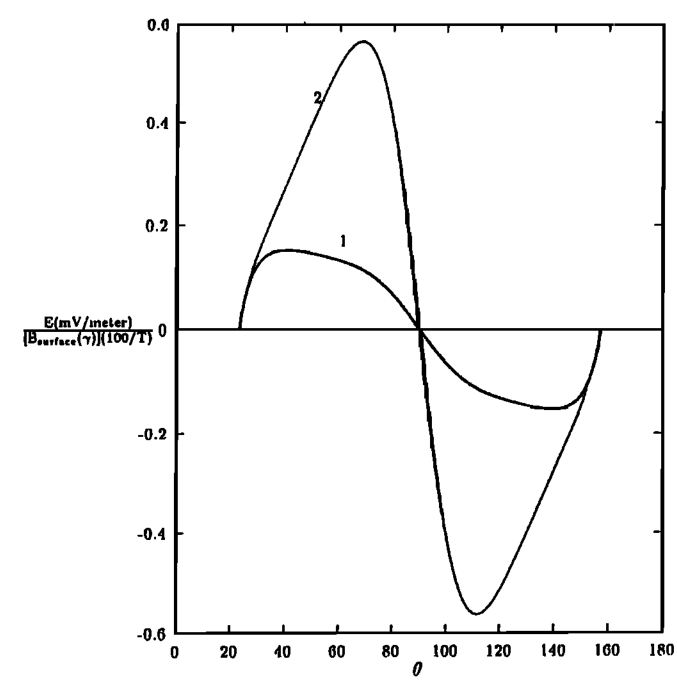

Figure 2c. The toroidal electric field for the second harmonic at any point along the field line for $m = 0$. Indices 1 and 2 have the same meaning as in Figure 2a.

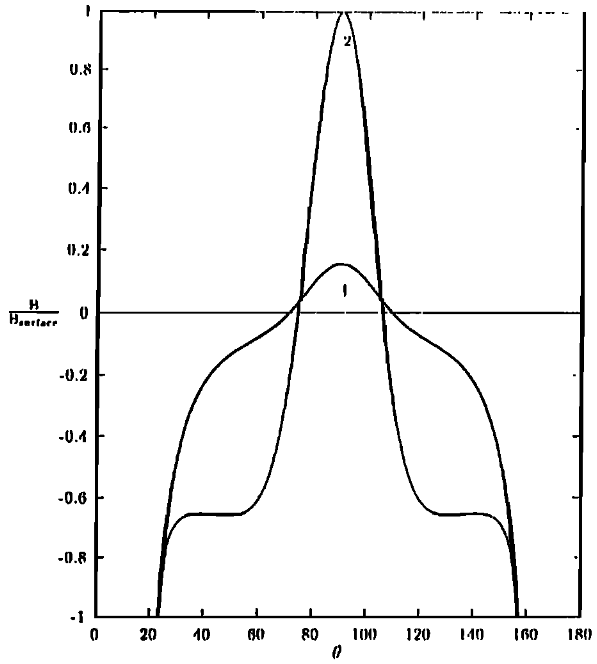

Figure 2d. The toroidal magnetic field for the second harmonic at any point along the field line for $m = 0$. Indices 1 and 2 have the same meaning as in Figure 2a.

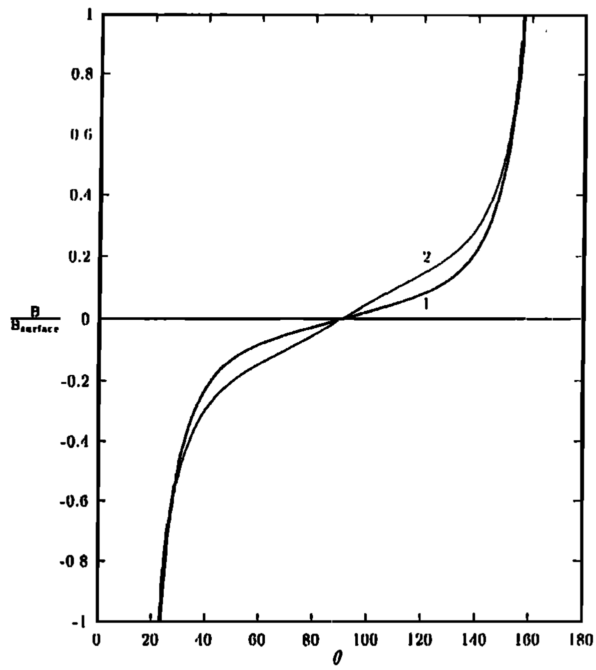

Figure 3b. The fundamental toroidal magnetic field at any point along the field line for $m = 4$. The value can be obtained in the same way as described in Figure 2b. Indices 1 and 2 have the same meaning as in Figure 2a.

If these singularities were not handled properly, the error caused in calculating the displacement of plasma will be carried all through the latitude thereby making the solution physically unrealistic. The present analytic method, where the effect due to the singularities at the turning points have been taken into account, shows a remarkable improvement in the frequency estimate as evident from Table-1. Even for the worst case (i.e., $m = 0$, fundamental mode) though the frequency is off by 17%, the eigen function differs by a fourth decimal place from the exact values. The discrepancies are much

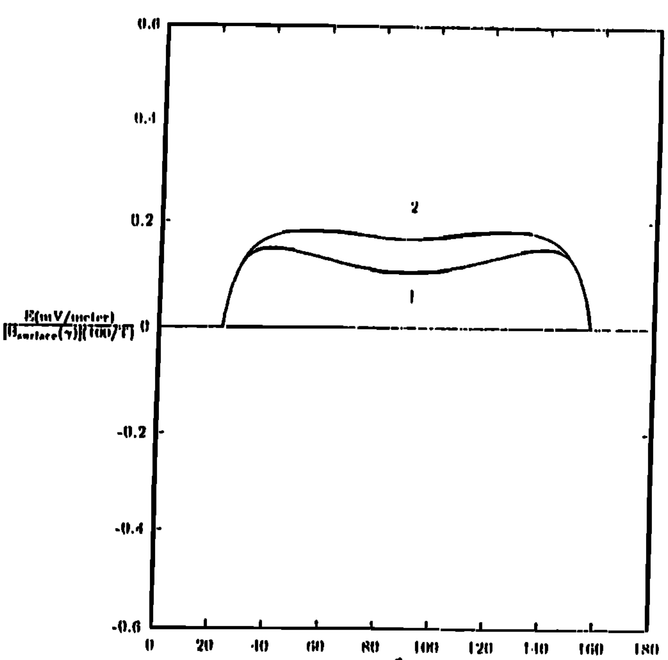

Figure 3a. The fundamental toroidal electric field at any point along the field line for $m = 4$. The value can be obtained in the same way as described in Figure 2a. Indices 1 and 2 have the same meaning as in Figure 2a.

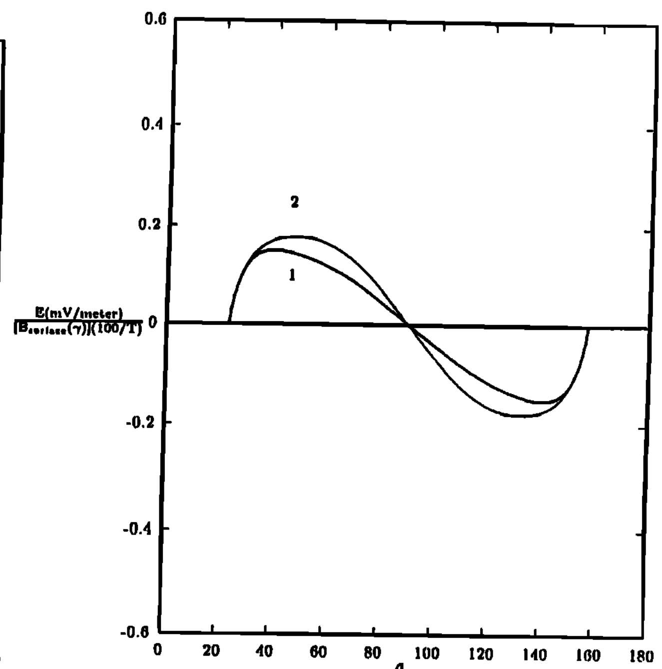

Figure 3c. The toroidal electric field for the second harmonic at any point along the field line for $m = 4$. The value can be obtained in the same way as described in Figure 2a. Indices 1 and 2 have the same meaning as in Figure 2a.

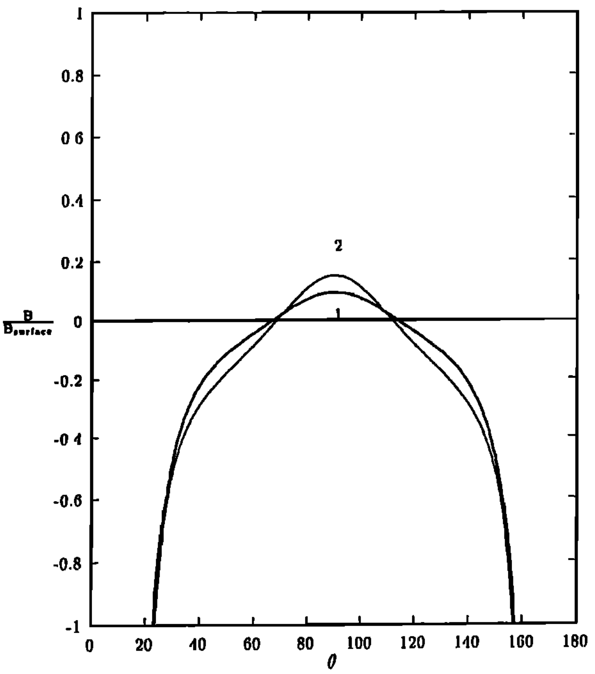

Figure 3d. The toroidal magnetic field for the second harmonic at any point along the field line for $m = 4$. Indices 1 and 2 have the same meaning as in Figure 2a.

less compared to the formal WKB method. For higher harmonics the frequency estimates are still better. The fundamental and second harmonic spatial structures of the electric and magnetic field fluctuations have been shown in Figures 2a-2d, 3a-3d, and 4a-4d typically for

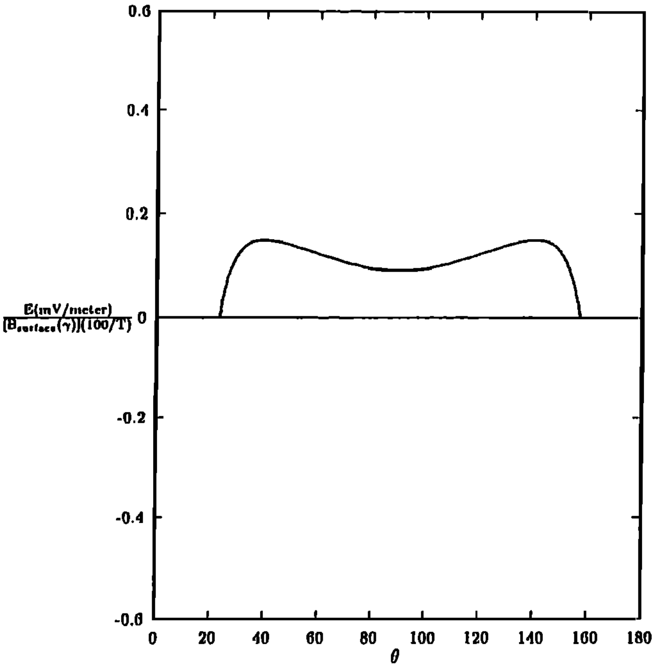

Figure 4a. The fundamental toroidal electric field at any point along the field line for $m = 6$. Here all three solutions, that is, exact solution, formal WKB solution, and direct analytic solution exactly coincide.

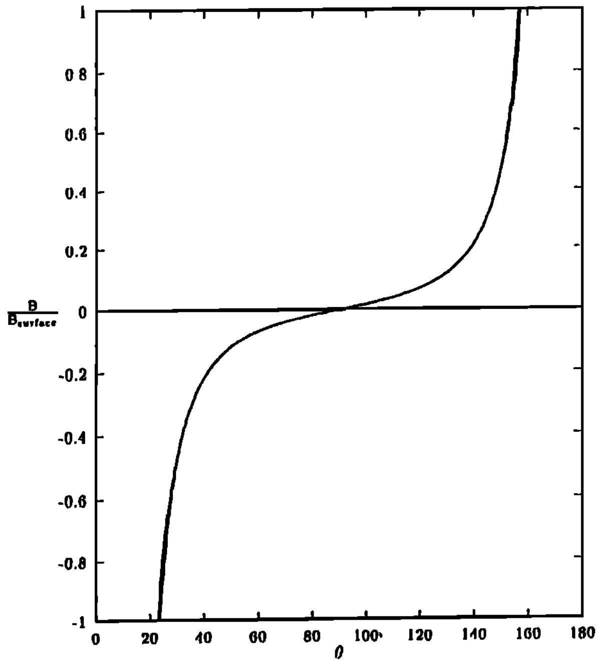

Figure 4b. The fundamental toroidal magnetic field at any point along the field line for $m = 6$. Here all three solutions, that is, exact solution, formal WKB solution, and direct analytic solution exactly coincide.

three values of m (i.e., $m = 0$, $m = 4$, and $m = 6$). The comparison shows that where the formal WKB solution, direct analytic solution, and numerical exact solution coincide exatly for $m = 6$, the formal WKB solution worsens for lower values of m but the direct analytic solution coincides with the numerically exact solution

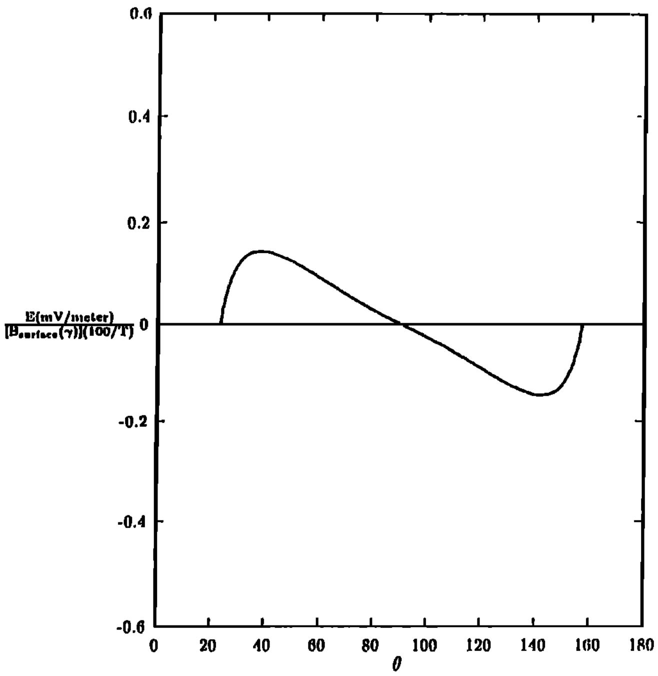

Figure 4c. The toroidal electric field for the second harmonic at any point along the field line for $m = 6$. Here all three solutions coincide.

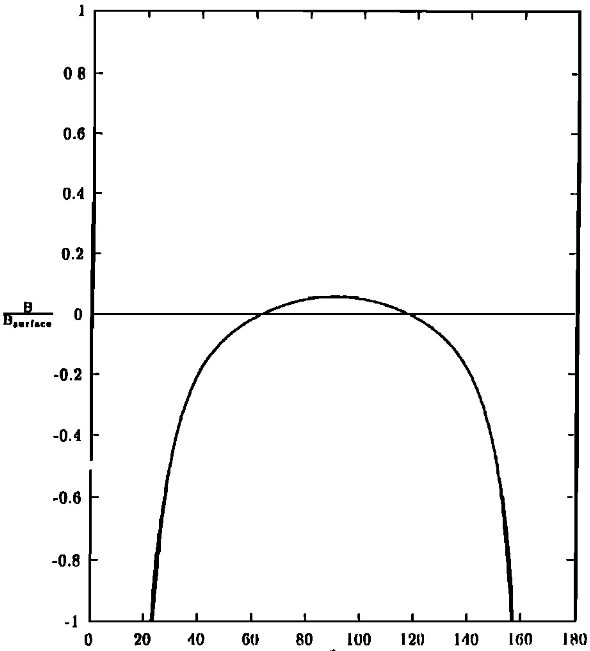

Figure 4d. The toroidal magnetic field for the second harmonic at any point along the field line for $m = 6$. Here all three solutions coincide.

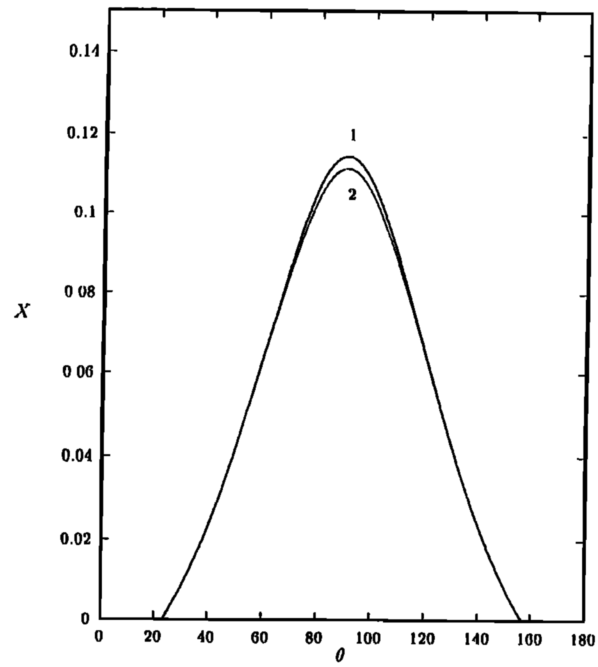

Figure 5. The plots of X for $m = 0$ as a function of colatitude θ. Index 1 represents the solution of equation (21), and index 2 represents the solution of equation (14)

for all values of m. This result has been very well depicted in the Figures 2a-2d, 3a-3d, and 4a-4d. Whereas the discrepancies in WKB solutions are very large for $m = 0$, it improves considerably for $m = 4$, and coincides exactly with the exact solution for $m = 6$. This is understandable because the dominance of turning point effect decreases with increasing value of m. The coincidence of the present analytic solution with the numerically found exact solution in spite of the small discrepancies in the frequency shows that the eigen function is not very sensitive to the frequency. It was seen for the worst case, $m = 0$, that maximum discrepancy of 3% in the eigen function (Figure 5) is equivalent to 22% discrepancy in the frequency.

4. Conclusions

The advantages of the discussed methodology are manifold as it provides solutions in a more natural way regarding the physics of the problem. Also, the correct analytic solution will prove to be important in understanding the phenomena of field line resonances in a more general way as the theory can be extended to more realistic nondipolar ambient field geometry and can incorporate more general density distribution other than the conventional power law. The small current leaking through the ionosphere along a field line can be computed by extending the boundary in the ionosphere. Moreover, the problems such as precipitations, diffusion, etc., where the field line structures play an important role, can be tackled with great ease without undergoing tedious computational work. The methodology can also be applied to other planets where the models for ambient magnetic field and the density distribution are known.

We strongly believe that the small discrepancies in the frequency can be rectified by taking higher-order correction into account. The work along this line is already in progress.

Acknowledgment. The editor thanks M. A. Termerin and another referee for their assistance in evaluating this paper.

References

Cummings, W. D., R. J. O'Sullivan, and P. J. Coleman, Standing Alfven waves in the magnetosphere, *J. Geophys. Res., 74,* 778, 1969.

Dungey, J. W., Electrodynamics of the outer atmospheres, *Rep. 69,* Ions. Res. Lab. Pa. State Univ., University Park, 1954.

Langer, R. E., The asymptotic solutions of ordinary linear differential equations of the second order, with special reference to a turning point, *Trans. Am. Math. Soc., 67,* 461, 1949.

McEntire, R. W., E. P. Keath, D. E. Fort, A. T. Y. Lui, and S. M. Krimigis, The Medium-Energy Particle Analyzer (MEPA) on the AMPTE CCE Spacecraft, *IEEE Trans. Geosci. Remote Sens., GE 23,* 230, 1985.

Mead, G. D., and D. H. Fairfield, A quantitative magnetospheric model derived from spacecraft magnetometer data, *J. Geophys. Res., 80,* 523, 1975.

Nagata, T., S. Kokubun, and T. Ijima, Geomagnetically conjugate relationships of giant pulsations at Syowa Base, Antarctica, and Reykjavik, Iceland, *J. Geophys. Res., 68,* 4621, 1963.

Singer, H. J. , D. J. Southwood, R. J. Walker, and M. G.

Kivelson, Alfven wave resonances in a realistic magnetospheric magnetic field geometry, *J. Geophys. Res.*, *86*, 4589, 1981.

Sugiura, M. , Evidence of low frquency hydromagnetic waves in the exosphere, *J. Geophys. Res.*, *66*, 4087, 1961.

Warner, M. R. , and D. Orr , Time of flight calculations for high latitude geomagnetic pulsations, *Planet. Space Sci.*, *27*, 679, 1979.

Wasow, W., *Linear Turning Point Theory*, 7 pp., Springer-Verlag, New York Inc., 1985.

A. K. Sinha and R. Rajaram, Indian Institute of Geomagnetism, Dr. Nanabhoy Moos Marg, Colaba, Mumbai 400 005. (e-mail: ashwini@iigm0.ernet.in; rajaram@iigm0.ernet.in)

(Received August 26, 1996; revised March 7, 1997; accepted April 3, 1997.)